Research Article

Pathumwan Academic Journal Vol. 13 ● No. 36 • January - April 2023

Improvement of APWM Switching Function with Positive Saw-tooth Waveform for AC Choppers

Chuthong Summatta[1] and Somchat Sonasang[2,*]

Received: 24 May 2022
Revised: 14 January 2023
Accepted: 10 February 2023

ABSTRACT

In AC chopper circuits, the improvement of the input power factor is the Asymmetrical Pulse Width Modulation (APWM). The modulation signal of APWM has two conventional operation driving modes for ac chopper circuit. This paper presents the improvement of the APWM switching function with a positive saw-tooth waveform for AC choppers. Where the reference signal can be increased or decreased at $\omega t = 0$ and fixed at $\omega t = \pi$. The developed method can also improve the carrier signal from the triangle signal to a positive saw-tooth signal and keep the trigger switching angle (α) constant throughout. The THD_{vo}, THD_{ii}, and PF_i results are performed by the Scilab and the Pspice computer simulation program. The comparisons to PWM and conventional APWM are also included.

Keywords: APWM; AC chopper; Switching function; Ac- Ac converter

[1]Department of Industrial Electrical Technology, Faculty of Industrial Technology, Nakhon Phanom University, Nakhon Phanom, Thailand, 48000

[2] Department of Electronic Technology, Faculty of Industrial Technology, Nakhon Phanom University, Nakhon Phanom, Thailand, 48000

[*] Corresponding author e-mail: somchat.s@npu.ac.th

Introduction

Now a day, the most connected load of the distribution power system is non-linear electricity loads. Also, these loads require different input voltage levels. Therefore, the waveform of the power system is an undesirable sinusoidal signal. The voltage and current harmonics occur in the power system. These harmonics cause voltage and current distortion, resulting in low power component values and loss of energy. Consequently, it is most necessary to use a converter circuit such as PWM controlled AC-AC converter in the distribution power system.

Typically, the power transfer using a PWM controlled AC-AC converter directly affects the input power element, thus it consists of the load power component and the AC-AC converter power component. Especially, the input of an AC-AC converter with PWM control, there are two methods: (1) designing the optimal parameters by analyzing the phase angle of the output voltage, output current and input current and (2) improving the PWM signal by considering the input power component, output voltage and total harmonic output voltage distortion [1-3]. Consequently, the improving power factor can be done by improving the PWM signals. Normally, there are two types of improvements in power components by improving the PWM signals as reported in previous studies such as the reference signal improvements and the carrier signal improvements. This modulates the PWM signal to shift the phase angle of the output voltage as an asymmetrical PWM (APWM) with zero voltage switching (ZVS) [4–8].

The APWM ideal switching function has two conventional operation modes with asymmetrical sawtooth waveform considered during an interval ($0, \pi$) such as constant slope mode and various slope modes [1-6]. Recently, a new alternative APWM using the slope reference is presented [7] whose amplitude is adjusted according to load requirements with the end of the signal fixed at $\omega t - \pi$. In this modulation, the signal remains positive. However, the input power component affects the efficiency of power transfer from the supply to the load and the timing of switching at an angle of 0 - 90 degrees, which makes the switching pattern. Therefore, in this research, a technique for improving the APWM signal is proposed. Also, the appropriate period in switching is determined taking into account the input power component, output voltage and the distortion of the total harmonic output voltage. To find a suitable answer, the input power factor of the converter circuit must approach one.

This paper presents the developed operation mode where the reference signal can be increased or decreased at $\omega t = 0$ and fixed at $\omega t = \pi$. The carrier signal is also improved from the triangle signal to a positive saw-tooth signal to keep the trigger switching angle (α) constant throughout. A comparison of the THD_{vo}, THD_{ii}, and PF_i values is made between the conventional PWM, APWM and the proposed APWM. The circuit results are performed by the Scilab and the Pspice computer simulation program.

Research and Methodology

The simple AC-AC converter or AC Chopper circuit controlled by pulse width modulation is shown in Figure 1. It employs switch S_1 to regulate and transfer electricity from the AC power source to the load. Consequently, switch S_2 is the free-wheeling path used to transfer the stored energy to the output load.

As shown in Figure 1, for the conventional APWM, the ideal switching function of the conventional APWM has two operation modes with a sawtooth waveform considered during the interval. The first mode is constant slope as shown in Figure 2(a) where the slope is fixed while the signal elevation is adjusted resulting in the average of X_o. On the other hand, the second mode is the various slope as shown in Figure 2(b) where the pivot point at position $\pi/2$ is fixed by adjusting the signal level up or down, causing the slope to change.

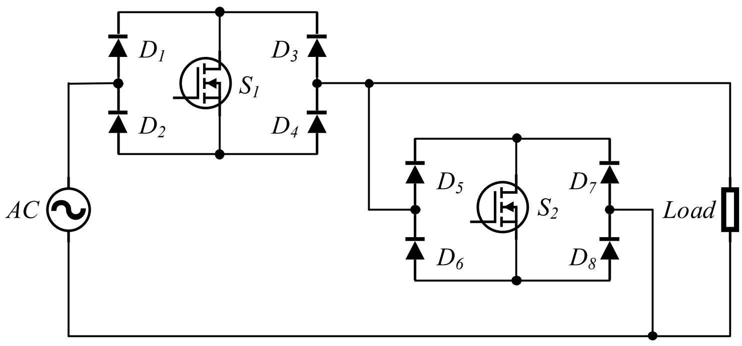

Figure 1 A single-phase AC chopper circuit.

As shown in Figure 2, the conventional ideal switching function operation modes can be expressed by Equation (1).

$$S(t) = -SL \cdot \omega t + B \tag{1}$$

Where B is the magnitude at $\omega t = 0$

C is the magnitude of S at $\omega t = \pi$

$$SL = B - \frac{B - C}{\pi} \tag{2}$$

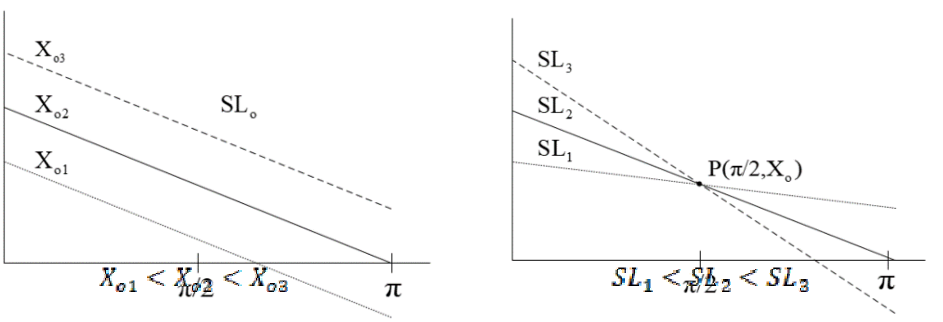

(a) The constant slope mode (b) The various slope mode

Figure 2 The conventional ideal switching function operation modes.

The concept of the switching function in previous publications [1-6] is to employ the slope reference that can be adjusted by increasing or decreasing the amplitude leading to an adjustment in the slope and the average signal level for load requirements with the end of the signal at π as shown in Figure 3. From equation 1, C is set only to zero at $\omega t = \pi$. The ideal switching function of S can be expressed by Equation (3).

$$S(t) = B - \frac{B}{\pi}\omega t \tag{3}$$

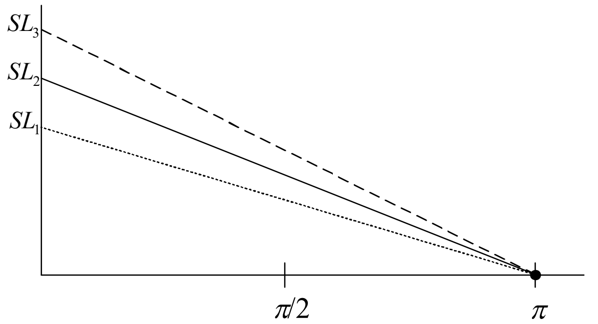

$SL_1 < SL_2 < SL_3$ and $X_o = B/2$

Figure 3 The operation modes of the ideal switching function.

The slope S and the constant B in the paper [7] method is varied to control the phase shift angles. Then, the average $X_o = B/2$ is changed for magnitude control of the output voltage and the slope SL for the phase shifting angle control.

From the articles mentioned above, the use of a negative saw-tooth slope reference signal with a triangular carrier signal is used. When the reference signal changes the level, the pulse signal S_1 with the start angle and the stop angle changes as shown in Figure 4. For ease of operation and calculations, the carrier signal has been modified to a positive saw-tooth signal so that the trigger angle can be determined based on the number of pulses in the range $0 - \pi$. The pulse signal $M = 6$ is determined, resulting in a trigger angle of $\alpha_1 = 0^o, \alpha_2 = 30^o, \alpha_3 = 60^o, \alpha_4 = 90^o, \alpha_5 = 120^o, \alpha_6 = 150^o$, as shown in Figure 5.

From Equation (3), it can be converted to the slope equation as follows:

$$y = -\frac{B}{m}x + B \tag{4}$$

where y is a function of the slope.
x is the coordinate in the x-axis.
B is the amplitude of the slope at the y-axis.
m is the number of carrier pulses in the interval $0 - \pi$.

$$y_i - x - i \; ; \; i \in \{1,2,\ldots,n\} \tag{5}$$

$$i = m_n - 1 \tag{6}$$

$$x_i = m_i\left(\frac{m}{m+1}\right) \tag{7}$$

Where m_i is the order of the sawtooth signal.

$$x_i = m\left(\frac{B + m_i - 1}{B + m}\right) \tag{8}$$

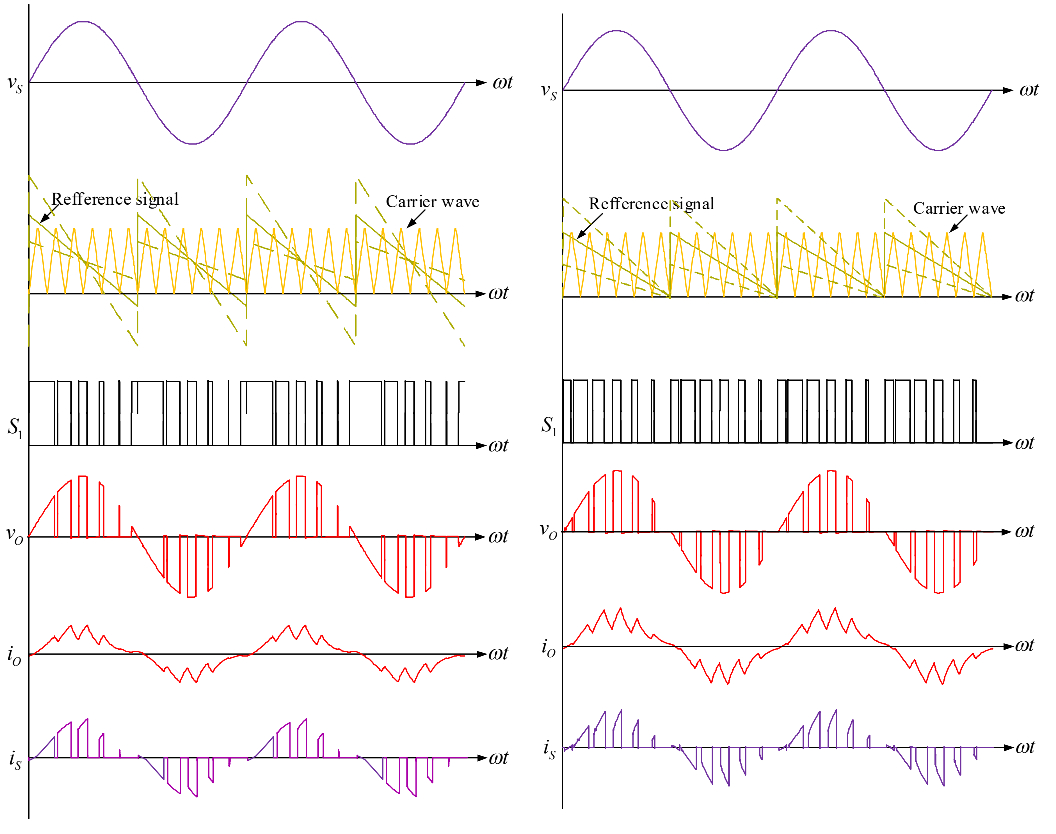

a) APWM mode 1 and 2 b) APWM mode 3

Figure 4 The waveforms of the switching function, output voltage, input current and output current.

Given that the sawtooth signal has an angle of 45, the equation of the sawtooth signal is

$$y = x - (m_i - 1) \tag{9}$$

Therefore, the intersection of the curves from Equations (4) and (9) determines the value of β.

$$\beta_i = x_i \frac{\pi}{m} \tag{10}$$

$$\therefore \beta_i = \pi\left(\frac{B + m_i - 1}{B + m}\right) \tag{11}$$

Where β_i is the turned-off angle of the pulse signal at the order position of the sawtooth signal. The objective of the function is to keep the size of THD to a minimum, which can be obtained from the equation (12).

$$\min_{\alpha,\beta} F = \sqrt{\left(A_1 - V_{o,ref}\right)^2 + A_3^2 + A_5^2 + \cdots + A_n^2} \quad (12)$$

Where A_1 is the fundamental coefficient of the output voltage.

$V_{o,ref}$ is the reference output voltage.

$$0 \le \alpha_1 \le \beta_1 \le \alpha_2 \le \beta_2 \le \cdots \le \alpha_m \le \beta_m;\ \beta_m \le \pi \quad (13)$$

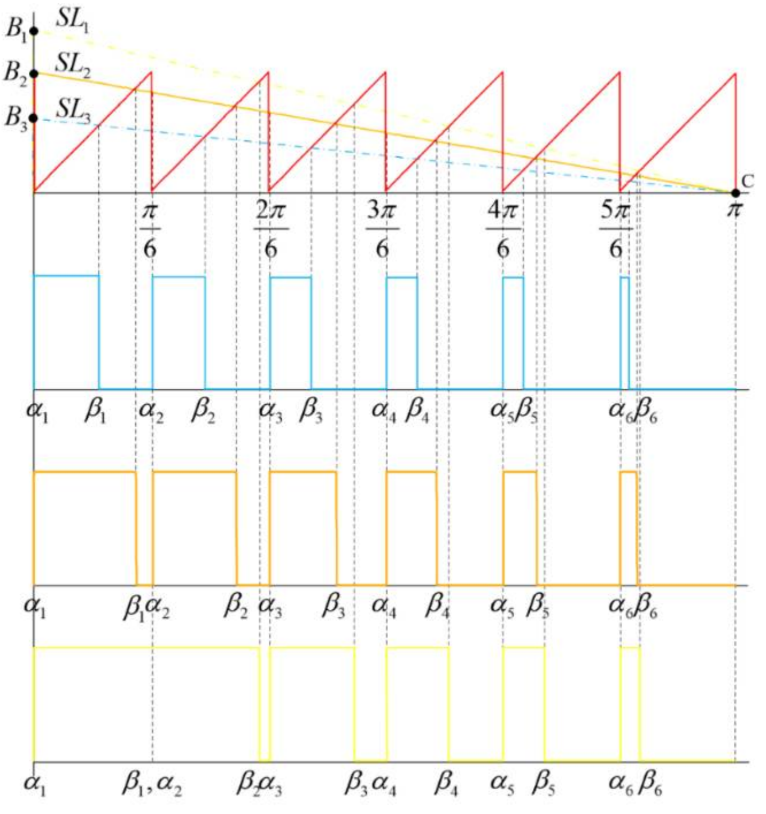

Figure 5 The proposed operation modes of the ideal switching function with a positive sawtooth carrier wave.

When the number of pulses in the range $0-\pi$ is six ($m = 6$), the boundary of the switch angle is

$$m_1 - \quad 0 \le \alpha_1 \le \beta_1 \le \pi/6$$
$$m_2 - \quad \pi/6 \le \alpha_2 \le \beta_2 \le 2\pi/6$$
$$m_3 - \quad 2\pi/6 \le \alpha_3 \le \beta_3 \le 3\pi/6$$
$$m_4 - \quad 3\pi/6 \le \alpha_4 \le \beta_4 \le 4\pi/6$$

$$m_5 = 4\pi/6 \le \alpha_5 \le \beta_5 \le 5\pi/6$$
$$m_6 = 5\pi/6 \le \alpha_6 \le \beta_6 \le 6\pi/6$$

An appropriate pulse signal form, as in equation (14), is used to design a converter circuit to reduce the THD, which requires a suitable operator to solve the problem.

$$v_o(\omega t) = \sum_{n=1}^{\infty}\{A_n sin(n\omega t) + B_n cos(n\omega t)\} \quad (14)$$

$$A_n = \frac{\sqrt{2}V_s}{\pi}\sum_{k=1}^{M}\left[\frac{sin\{(n-1)\beta_k\} - sin\{(n-1)\alpha_k\}}{(n-1)} - \frac{sin\{(n+1)\beta_k\} - sin\{(n+1)\alpha_k\}}{(n+1)}\right] \quad (15)$$

$$B_n = \frac{\sqrt{2}V_s}{\pi}\sum_{k=1}^{M}\left[\frac{cos\{(n-1)\beta_k\} - cos\{(n-1)\alpha_k\}}{(n-1)} - \frac{cos\{(n+1)\beta_k\} - cos\{(n+1)\alpha_k\}}{(n+1)}\right] \quad (16)$$

The output of the equation is written in the Fourier equation.

$$v_o(\omega t) = \sum_{n=1}^{\infty} C_n sin\{n\omega t + \emptyset_{R_n}\} \quad (17)$$

Where

$$C_n = \sqrt{A_n^2 + B_n^2} \quad (18)$$

$$\emptyset_{R_n} = tan^{-1}\frac{B_n}{A_n} \quad (19)$$

Therefore, the load current output equation can be obtained by Equation (20).

$$i_o(\omega t) = \sqrt{2}V_s \sum_{n=1}^{\infty}\frac{C_n}{\sqrt{R^2 + (nX)^2}} sin\{n\omega t + \emptyset_{R_n} + \emptyset_{on}\} \quad (20)$$

$$\emptyset_{on} = tan^{-1}\frac{nX}{R} \quad (21)$$

Given that I_{on} and V_{on} are the RMS values of the n^{th} harmonics of the output current and the output voltage, respectively, the THD equations of the output current and voltage are possible.

$$THD_i = \frac{\sqrt{\sum_{n=3}^{\infty} I_{on}^2}}{I_{o1}} \quad (22)$$

$$THD_v = \frac{\sqrt{\sum_{n=3}^{\infty} V_{on}^2}}{V_{o1}} \quad (23)$$

Where n = 3,5,7,... Therefore, the input power factor equation can be obtained by.

$$PF_i = \frac{cos\,\emptyset_{in}}{\sqrt{1 + THD_i^2}} \quad (24)$$

Results and Discussion

The proposed APWM switching function for AC choppers is designed and simulated by computer simulation. The simulation results for the single-phase AC chopper by determining the R-L load with a fixed value at $Z = 240 + j314$ are shown in Figure 6. The number of carrier pulses in the interval $0 \quad \pi$ is six ($m = 6$). The voltage supply to the circuit is 220 V_{rms} at 50 Hz.

From Figure 6, the initial amplitude of the reference signal was set to 4.5 volts, the carrier amplitude was 5 volts, and the output voltage was approximately 150 V_{rms}.

The operation to determine the tune-on angle (α) and the tune-off angle (β) is simulated by setting the output voltage in the range of every 20 V from 20 to 200 V by comparing the conventional APWM and the proposed APWM, shown in Table 1 and Table 2.

The turn-on and turn-off switching angles at various output voltage levels for controlling the PWM AC Chopper are simulated by the Scilab computer program. The simulation results are carried out in the Pspice program environment for the single-phase AC chopper by determining the fixed R-L load $(Z = 240 + j120)$. The voltage source to the circuit is 220 V_{rms} at 50 Hz.

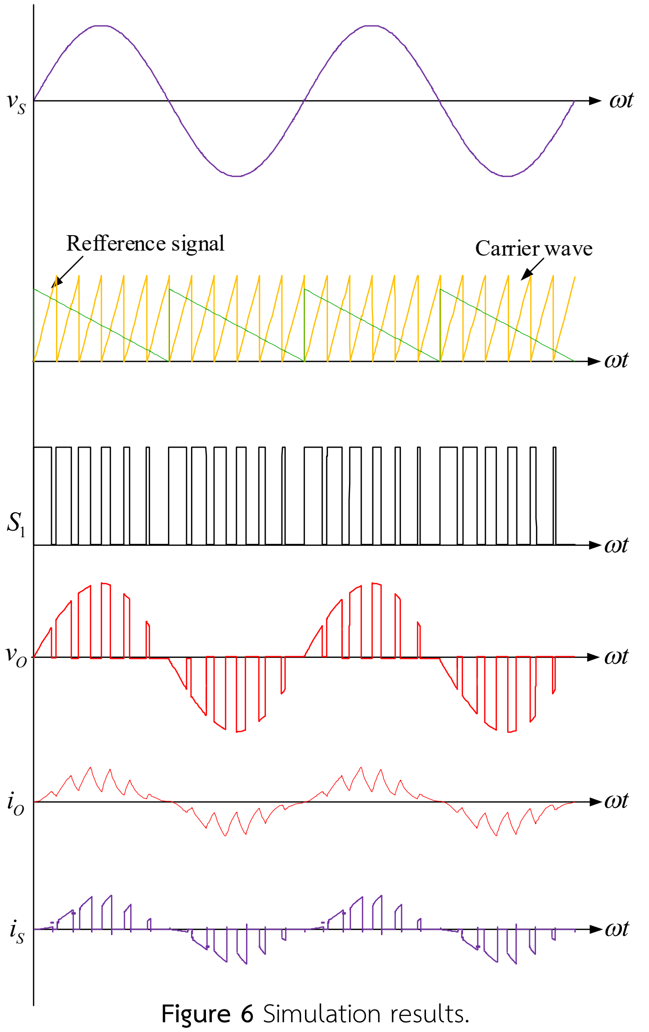

Figure 6 Simulation results.

Table 1 The turn-on and turn-off switching angles of the Proposed APWM at various output voltage levels

Output Voltage $V_o(V)$	The switching angle (degree)											
	α_1	β_1	α_2	β_2	α_3	β_3	α_4	β_4	α_5	β_5	α_6	β_6
20	0	0.47	30	30.59	60	60.31	90	90.23	120	120.15	150	150.07
40	0	1.78	30	31.48	60	61.18	90	90.89	120	120.59	150	150.29
60	0	4.10	30	33.42	60	62.73	90	92.05	120	121.36	150	150.68
80	0	7.47	30	36.23	60	64.98	90	93.73	120	122.49	150	151.24
100	0	11.25	30	39.37	60	67.50	90	95.62	120	123.75	150	151.87
120	0	16.36	30	43.63	60	70.90	90	98.18	120	125.45	150	152.72
140	0	21.17	30	47.64	60	74.11	90	100.58	120	127.05	150	153.52
160	0	27.88	30	53.23	60	78.59	90	103.94	120	129.29	150	154.64
180	0	34.05	30	58.37	60	82.70	90	107.02	120	131.35	150	155.67
200	0	43.97	30	66.64	60	89.31	90	111.98	120	134.65	150	157.32

Table 2 The performance of the APWM at various output voltage levels

Output Voltage $V_o(V)$	Conventional PWM			APWM			Proposed APWM		
	PF_i	THD_{io}	THD_{vo}	PF_i	THD_{io}	THD_{vo}	PF_i	THD_{io}	THD_{vo}
20	0.3467	0.2682	2.4110	0.8925	0.0493	0.3151	0.8949	0.0546	1.6716
40	0.3755	0.2496	1.9635	0.6447	0.0952	0.7953	0.7747	0.0628	1.0978
60	0.4270	0.2296	1.5297	0.8879	0.0971	0.3399	0.5233	0.0804	1.0398
80	0.4816	0.2104	1.2324	0.8871	0.0992	0.3202	0.8894	0.0897	0.2271
100	0.5485	0.1933	1.0345	0.8661	0.1025	0.1310	0.8795	0.0929	0.3124
120	0.6000	0.1779	0.8625	0.8787	0.0972	0.1204	0.8686	0.0892	0.1926
140	0.6827	0.1630	0.6901	0.8741	0.0962	0.1734	0.8771	0.0904	0.1373
160	0.7290	0.1515	0.5637	0.8596	0.0933	0.1488	0.8604	0.0942	0.1435
180	0.7594	0.1422	0.4156	0.8608	0.1347	0.1865	0.8546	0.0904	0.2198
200	0.7866	0.1363	0.2054	0.8546	0.0949	0.1767	0.8668	0.0962	0.1272

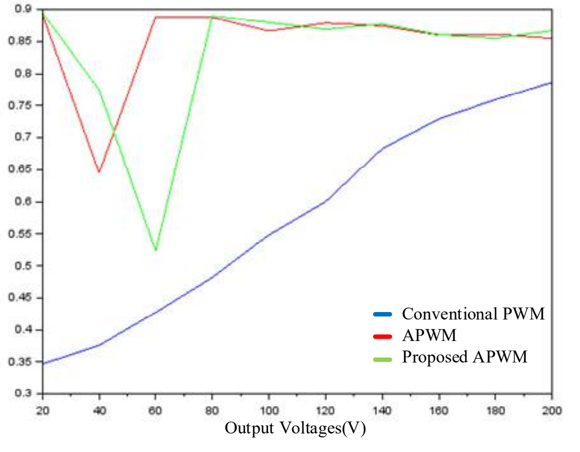

(a) Input power factor

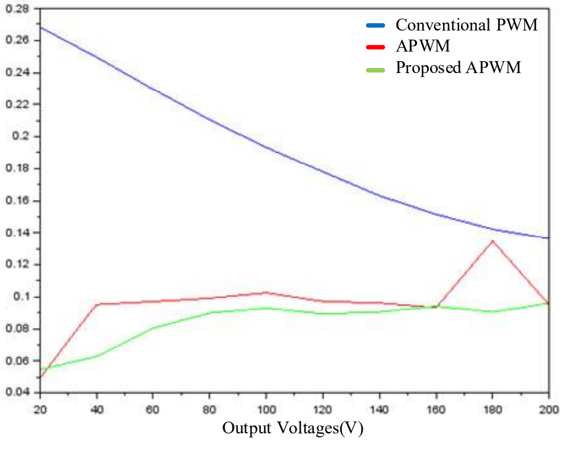

(b) Total harmonic distortion of output current

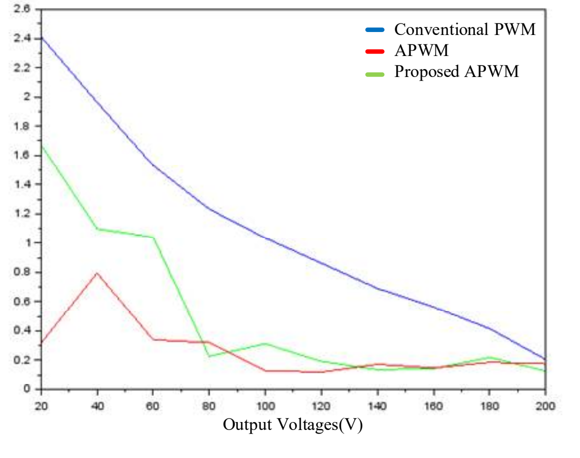

(c) Total harmonic distortion of output voltage

Figure 7 PF_i, THD_{io}, THD_{vo} versus various output voltages.

Table 1 shows the turn-on and turn-off switching angles of the APWM method presented at different output voltages from 20–200 V. The proposed method has a constant turn-on angle and the turn-off angle increases linearly as the output voltage increases, which can be used to find the input power factor, total harmonic distortion of output current and total harmonic distortion of output voltage as shown in Table 2.

Table 2 compares PF_i, THD_{io}, THD_{vo} for the three methods of conventional pulse with modulation, asymmetrical pulse with modulation and proposed asymmetrical pulse with modulation.

The simulation results of the proposed APWM method can be compared to the two standard methods and APWM in the paper [7]. In figures 7(b) and 7(c), the THD_{io} and THD_{vo} are significantly lower when compared with the other techniques for different output voltage levels. Figure 7(b), the PF_i of the proposed APWM technique is similar to that of the other APWM but higher than the conventional PWM technique.

Conclusion

This paper presents the application of the Asymmetrical Pulse Width Modulation (APWM) method for improving the input power factor in ac chopper circuits. The developed operation mode whose reference signal can be increased or decreased at $\omega t - 0$ and fixed at $\omega t - \pi$. The developed method can also improve the carrier signal from the triangle signal to a positive saw-tooth signal keeping the trigger switching angle (α) constant throughout. The performance of PF_i, THD_{vo}, and THD_{ii} of the proposed APWM is compared with those of the conventional PWM and APWM. The performance of the proposed APWM technique is considered at the fixed R-L load ($Z = 240 + j120$). The voltage supply to the circuit is 220 V_{rms} at 50 Hz. The circuit results are performed by the Scilab and Pspice program.

Acknowledgment

Thank you, Research and Development Institute Nakhon Phanom University for supporting this work.

References

[1] Sagar, R. A., & Reddy, B. V. (2012). Comparative analysis of SPWM and APWM techniques for three phase AC chopper. *International Journal of Emerging Trends in Engineering and Development*, 4, 230-237.

[2] Jang, D. H., et al. (1991). Asymmetrical PWM method for AC chopper with improved input power factor. In *PESC '91 Record 22nd Annual IEEE Power Electronics Specialists Conference* (p. 838-845). 24-27 June, 1991, Cambridge, MA, USA.

[3] Choe, G. H., & Jang, D. H. (1991). Asymmetrical PWM technique for AC choppers. In *1991 International Conference on Industrial Electronics, Control and Instrumentation* (p. 587-592). 28 October-1 November, 1991, Kobe, Japan.

[4] Jang, D. H., & Choe, G. H. (1995). Improvement of input power factor in AC choppers using asymmetrical PWM technique. *IEEE Transactions on Industrial Electronics*, 42(2), 179-185.

[5] Choe, G. H., et al. (1989). An improved PWM technique for AC choppers. *IEEE Transactions on Power Electronics*, 4(4), 496-505.

[6] Jang, D. H., et al. (1995). Asymmetrical PWM technique with harmonic elimination and power factor control in AC choppers. *IEEE Transactions on Power Electronics*, 10(2), 175-184.

[7] Summatta, C., et al. (2018). Improvement of Asymmetrical Pulse Width Modulation Switching Function for AC Chopper. In *2018 Electrical Engineering/Electronics, Computer, Telecommunications and Information Technology (ECTI-CON)* (p. 441-444). Changrai, Thailand.

[8] Khamsen, W., et al. (2011). Designing parameters in PWM buck AC chopper for unity input power factor. In *The 8th Electrical Engineering/ Electronics, Computer, Telecommunications and Information Technology (ECTI) Association of Thailand - Conference 2011* (p. 731-734). 17-19 May, 2011, Khon Kaen, Thailand.

[9] Khamsen, W., et al. (2013). Power factor improvement and voltage harmonics reduction in pulse width modulation AC chopper using bee colony optimization. *IETE Technical Review*, 30(3), 173-182.

[10] Khamsen, W., et al. (2014). Optimal switching pattern for PWM AC-AC converter using bee colony optimization. *Journal of Power Electronics*, 14(2), 362-368.

[11] Rashid, M. H. (1993). Power Electronics: Circuits, *Devices and Applications*. New Jersey: Prentice-Hall.

[12] Balci, M. E., & Hocaoglu, M. H. (2005). Effects of source voltage harmonic distortion on power factor compensation in triac controlled AC chopper circuits. In *2005 International Conference on Power Electronics and Drives Systems* (p. 1199-1204). 28 November - 01 December, 2005, Kuala Lumpur, Malaysia.

[13] Rao, S. S., & Shailaja, N. (2005). Improving voltage regulation and harmonic elimination using genetic algorithm in PWM choppers. In *27th International Telecommunications Conference* (p. 449-454). 18-22 September, 2005, Berlin, Germany.

[14] Al-Othman, A. K., et al. (2007). Selective harmonic elimination of PWM AC/AC voltage controller using hybrid RGA-PS approach. *Journal of World Academy of Science, Engineering and Technology*, 1(5), 140-146.

[15] Kitcharoenwat, S., et al. (2012). A novel single phase AC-AC converter with power factor control. In *9th International Conference on Electrical Engineering/Electronics,*

Computer, Telecommunications and Information Technology (p. 1-4). 16-18 May, 2012. Phetchaburi, Thailand

[16] Ashraf, N., et al. (2019). A Single-Phase Buck and Boost AC-to-AC Converter with Bipolar Voltage Gain: Analysis, Design, and Implementation. *Energies*, 12(7), 1376.

[17] Summatta, C., et al. (2019). Low-cost and Compact Window Comparator Circuit with MOSFET-Resistor Voltage References. In *IEEE 2nd International Conference on Power and Energy Applications (ICPEA)* (p. 75-78). 27-30 April 2019. Singapore.

[18] Summatta, C. & Sonasang, S. (2022). Safety analysis of 2-pin capacitor as 4-pin capacitor with frequency response. *SNRU Journal of Science and Technology*, 14(3), 1-6.

[19] Summatta, C., et al. (2016). Design and simulation of relay drive circuit for safe operation order. In *Conference on Mathematics, Engineering & Industrial Applications 2016 (Icomera 2016)* (p. 1-8). 10-12 August, 2016. Songkhla, Thailand.